Bioorganic & Medicinal Chemistry 20 (2012) 3460–3464

Contents lists available at SciVerse ScienceDirect

Bioorganic & Medicinal Chemistry

journal homepage: www.elsevier.com/locate/bmc

Bidirectional fluorescence properties of pyrene-based peroxisome proliferator-activated receptor (PPAR) α/δ dual agonist

Shintaro Ban [a], Takuji Oyama [b], Jun-ichi Kasuga [c], Kenji Ohgane [c], Yoshino Nishio [a], Kosuke Morikawa [d], Yuichi Hashimoto [c], Hiroyuki Miyachi [a,*]

[a] Graduate School of Medicine, Dentistry and Pharmaceutical Sciences, Okayama University, 1-1-1, Tsushima-Naka, Kita-ku, Okayama 700-8530, Japan
[b] Institute for Protein Research, 3-2, Yamadaoka, Suita, Osaka 565-0871, Japan
[c] Institute of Molecular and Cellular Biosciences, University of Tokyo, Yayoi, Bunkyo-ku, Tokyo 113-0032, Japan
[d] International Institute for Advanced Studies, 9-3, Kizugawadai, Kizugawa City, Kyoto 619-0225, Japan

ARTICLE INFO

Article history:
Received 3 March 2012
Revised 5 April 2012
Accepted 6 April 2012
Available online 16 April 2012

Keywords:
Peroxisome proliferator-activated receptor
PPARδ
PPARα
Fluorescent PPARα/δ co-agonist
Site-directed mutagenesis

ABSTRACT

Based on X-ray crystallographic analysis of a peroxisome proliferator-activated receptor (PPAR) α/δ dual agonist complexed with human PPARs ligand binding domain (LBD), we previously reported the design and synthesis of a pyrene-based fluorescent PPARα/δ co-agonist **2**. Here, we found that the fluorescence intensity of **2** increased upon binding to hPPARα-LBD, in a manner dependent upon the concentration of the LBD. But, surprisingly, the fluorescence intensity of **2** decreased concentration-dependently upon binding to hPPRδ-LBD. Site-directed mutagenesis of the two hPPAR subtypes clearly indicated that Trp264 of hPPARδ-LBD, located between H2′ helix and H3 helix (omega loop), is critical for the concentration-dependent decrease in fluorescence intensity, which is suggested to be due to fluorescence resonance energy transfer (FRET) from the pyrene moiety of bound **2** to the nearby side-chain indole moiety of Trp264 in the hPPARδ-LBD.

1. Introduction

Peroxisome proliferator-activated receptors (PPARs) are ligand-activated transcription factors that belong to the nuclear receptor superfamily.[1–3] They mediate pleiotropic biological responses, and have well-established regulatory roles in lipid, lipoprotein and glucose homeostasis.[4–6] PPARs are activated by endogenous fatty acids, especially unsaturated fatty acids such as eicosapentaenoic acid (EPA), docosahexaenoic acid (DHA), and synthetic agonists.[7] Three subtypes have been found to date: PPARα (NR1C1), PPARδ (NR1C2) and PPARγ (NR1C3),[8] and each subtype has a characteristic tissue distribution pattern.[9] PPARα is mostly expressed in tissues with high fatty acid catabolism activity, such as liver, kidney, skeletal muscle, cardiac muscle and adrenal glands.[10] PPARγ is expressed mainly in white and brown adipose tissue, macrophages and vascular smooth muscles.[11] In contrast, PPARδ is ubiquitously expressed.[12]

Two of these PPAR subtypes are well-known molecular targets of drugs used to treat type II diabetes mellitus and dyslipidemia, that is, the insulin-sensitizing glitazones, such as pioglitzone and rosiglitazone, are classical full agonists of PPARγ,[13] while the dyslipidemia-normalizing fibrate class of compounds, such as fenofibrate and bezafibrate, are weak agonists of PPARα.[14] On the other hand, the availability of PPARδ knockout animals and selective ligands led us to examine the involvement of PPARδ in fatty acid metabolism, insulin resistance, reverse cholesterol transport and inflammation.[15] Since activation of PPARδ was reported not only to improve glucose tolerance and insulin resistance, but also to restore embryo implantation,[16] myelination in the brain[17] and osteoclastic bone resorption,[18] there is increasing interest in this receptor subtype as a target for drug development.

For our research directed toward the structural development of subtype-selective human PPAR (hPPAR) agonists,[19–23] we needed a simple method to evaluate the hPPARδ binding activity of test compounds without the use of isotope-labeling, which has a variety of disadvantages. We proceeded to design and synthesize a fluorescent hPPARα/δ co-agonist **2**, which proved suitable for use in a homogeneous fluorescence polarization assay format.[24] The small planar fluorophore pyrene was selected based on the X-ray crystallographic structure of the complex of our hPPARα/δ co-agonist **1** with hPPARα ligand binding domain (LBD) (Fig. 1, PDB: 2ZNQ), in which the hydrophobic 2-fluoro-4-trifluoromethylphenyl group of **1** is located in the cavity of the Y-shaped pocket of hPPARα-LBD (Fig. 1).[25]

Examination of the fluorescence properties of **2** complexed with hPPARα-LBD afforded surprising results. We found that the fluorescence intensity of 500 nM **2** increased with increasing

* Corresponding author. Tel.: +81 086 251 7930.
E-mail address: miyachi@pharm.okayama-u.ac.jp (H. Miyachi).

0968-0896/$ - see front matter © 2012 Elsevier Ltd. All rights reserved.
http://dx.doi.org/10.1016/j.bmc.2012.04.015

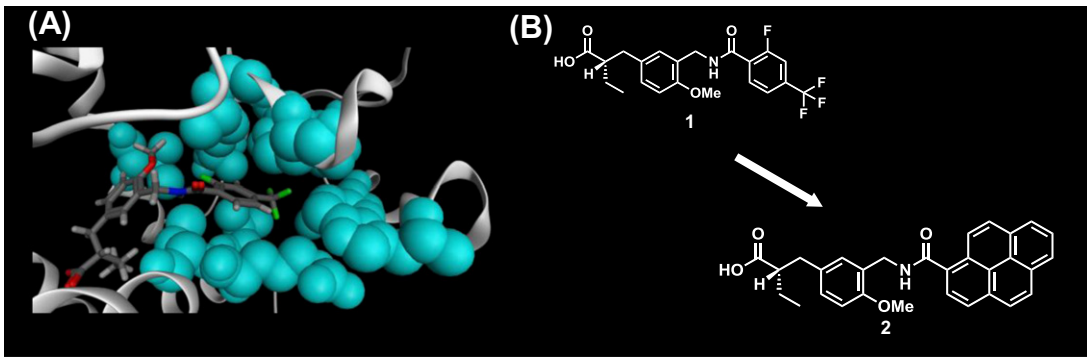

Figure 1. (A) Zoomed view of the binding mode of the hydrophobic tail part of **1** complexed with hPPARδ-LBD. Protein is represented as a white ribbon model and the surrounding amino acids are depicted as cyan space-filling models. **1** is depicted as a cylinder model. (B) Chemical structures of **1** and **2**.

concentration of hPPARα-LBD in binding buffer (Tris–HCl 20 mM, NaCl 150 mM, TCEP (tris[2-carboxyethyl]phosphine hydrochloride)1 mM, pH 7.5) (Fig. 2, top left), as expected. We confirmed that the combination of hPPARα-LBD and the binding buffer used did not show significant fluorescence. But, in the case of hPPARδ-LBD, **2** showed the opposite property, that is, the fluorescence intensity of 500 nM **2** decreased with increasing concentration of hPPARδ-LBD in binding buffer (Fig. 2, top right).

These bi-directional fluorescence properties of **2**, depending on complexation with either hPPARα-LBD or hPPARδ-LBD, are interesting, and in the present work we used point-mutated hPPARα-LBD and hPPARδ-LBD to examine the structural basis of this phenomenon.

2. Results and discussion

The fluorescence intensity of a fluorescent ligand is usually expected to increase upon binding to the target molecule because of the hydrophobic nature of the binding pocket, and in this context, the augmentation of the fluorescence of **2** upon binding to hPPARα-LBD is reasonable. Therefore, there must be a special explanation for the concentration-dependent attenuation of the fluorescence of **2** upon binding to hPPARδ-LBD.

Figure 3A–D shows the binding modes of **2** complexed with hPPARα-LBD (Fig. 3A and B)[26] and **1** complexed with hPPARδ-LBD (Fig. 3C and D).[25] The pyrene ring of **2** is buried in the Y2 arm of the hPPARα LBD, which is composed of the side chains of the amino acids Leu247, Glu251, Val255, Leu258, Ile272, Cys275, Thr279, Val332, Ala333 and Ile339. It is noteworthy that all these amino acids are aliphatic. However, in the case of the hPPARδ-LBD, the Y2 arm is composed of the side chains of Ile249, Leu255, Glu259, Trp264, Val281, Arg284, Val341, Val348, Phe352 and Leu353, that is, the Y2 arm of hPPARδ-LBD contains two aromatic amino acids, Trp264 and Phe352. The trifluoromethyl group of **1** is less than 2 Å away from Trp264, while it is more than 3.5 Å from Phe352. Therefore, the tryptophan residue might interact with the pyrene moiety of **2**, when **2** is bound to the hPPARδ-LBD.

The aromatic amino acids tryptophan, tyrosine and phenylalanine are all intrinsically fluorescent, but tryptophan is the most powerful fluorophore of the three, because tyrosine and phenylalanine have low excitation coefficients and low quantum yields.[27] We speculated that fluorescence quenching involving Trp264 might occur when **2** is excited in the complex with hPPARδ-LBD, that is, the fluorescence energy of the excited-state pyrene might be transferred to the nearby Trp264. There is another tryptophan residue in hPPARδ-LBD, that is, Trp256 (Fig. 3E), but this is located in the H2 helix and the side-chain indole residue faces outside of the hPPARδ-LBD, so it is unlikely to be involved in fluorescence quenching.

In order to test our working hypothesis, we constructed four mutant hPPARs-LBDs, that is, Trp264 of hPPARδ-LBD was changed to Leu (hPPARδW264L-LBD), and the corresponding Leu of hPPARα-LBD was changed to Trp (hPPARαL258W-LBD), Trp264 of hPPARδ-LBD was changed to Ala (hPPARδW264A-LBD), and Trp256 of hPPARδ-LBD was changed to Ala (hPPARδW256A-LBD). The effects of these mutated hPPAR-LBDs on the fluorescence properties of **2** were then examined.

As shown in Figure 4A–D, Trp264 but not Trp256 is required for the change of the fluorescence properties of **2**. The fluorescence intensity of **2** was augmented in the presence of increasing

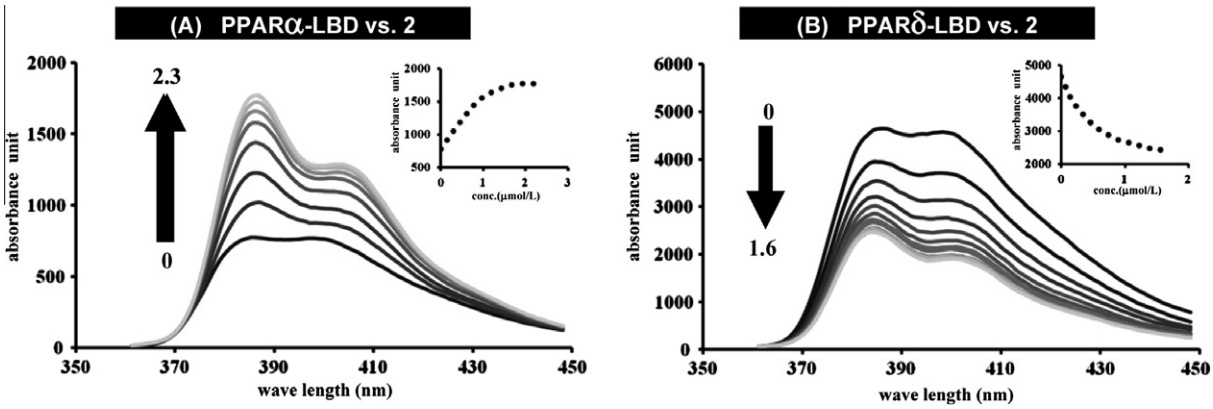

Figure 2. (A) Fluorescence spectra of 500 nM **2** during cumulative addition (0–2.3 μM) of hPPARα-LBD in binding buffer. Excitation and emission wavelengths were λ = 345 and 390 nM, respectively. (B) Fluorescence spectra of 500 nM **2** during cumulative addition (0–1.6 μM) of hPPARδ-LBD in binding buffer.

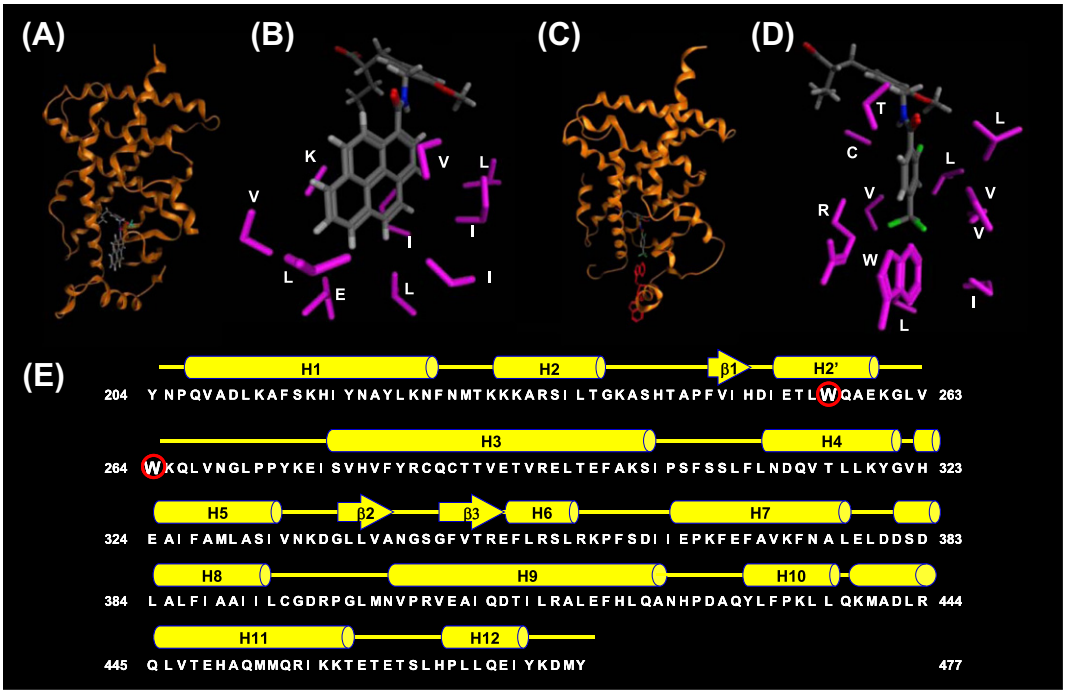

Figure 3. (A) hPPARα-LBD–**2** complex. Protein is represented as a brown ribbon model and the ligand is depicted as a cylinder model. (B) Zoomed view of the binding mode of the hydrophobic pyrene moiety of **2** in hPPARα-LBD–**2** complex. The surrounding amino acids are depicted as magenta cylinder models. (C) hPPARδ-LBD–**1** complex. Protein is represented as a brown ribbon model and the ligand is depicted as a cylinder model. (D) Zoomed view of the binding mode of the hydrophobic 4-trifluorophenyl moiety of **1** in the hPPARδ-LBD–**1** complex. The surrounding amino acids are depicted as magenta cylinder models. (E) Primary and secondary structures of hPPARδ-LBD. Helical regions are shown as yellow cylinders. Two tryptophan residues are circled in red.

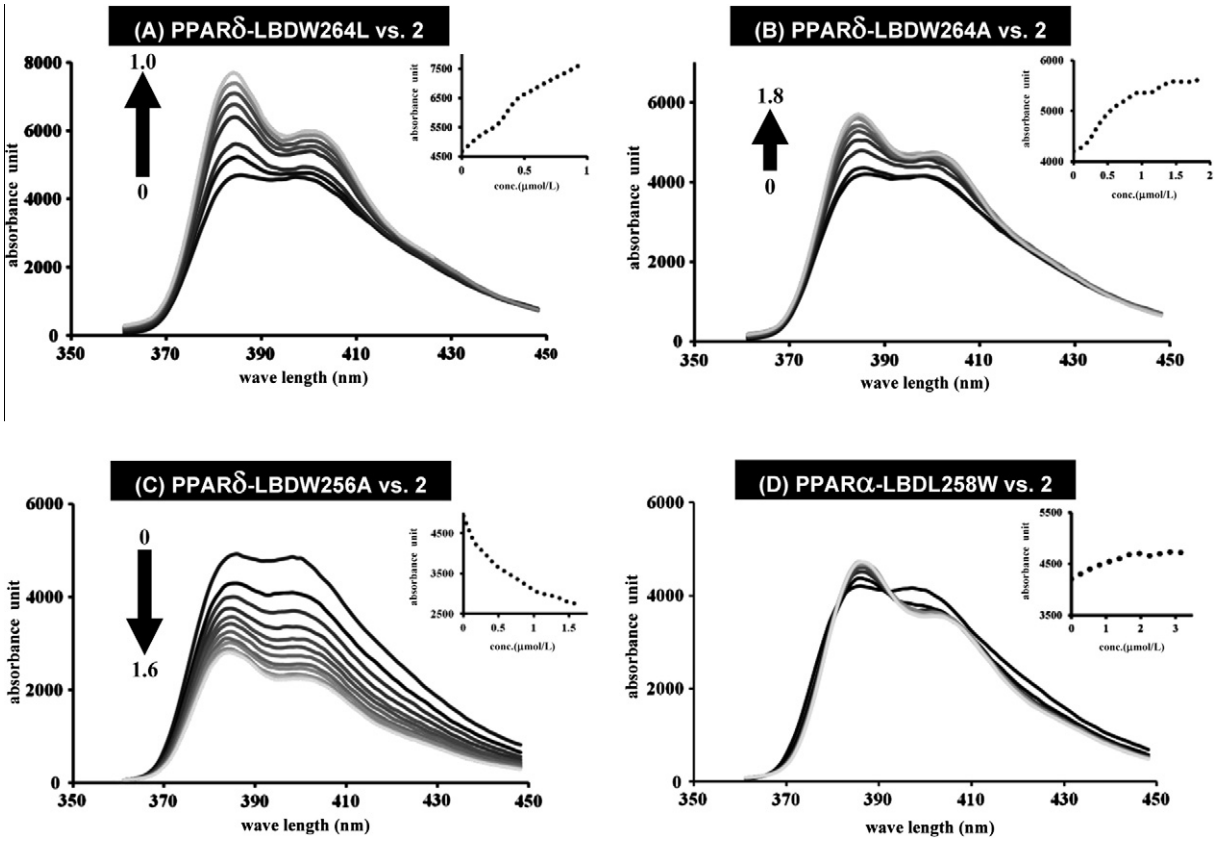

Figure 4. Fluorescence spectra of 500 nM **2** during cumulative addition of (A) hPPARδ264L-LBD 0–1.0 μM, (B) hPPARδW264A-LBD 0–1.8 μM, (C) hPPARδW256A-LBD 0–1.6 μM, and (D) hPPARα258 W-LBD 0–3.2 μM, each in binding buffer. Excitation and emission wavelengths were λ = 345 and 390 nM, respectively.

amounts of hPPARδW264L-LBD (0–0.97 μM) or hPPARδW264A-LBD (0–1.80 μM), while hPPARδW256A-LBD did not affect the fluorescence of **2**. The fluorescence of **2** was decreased in the presence of increasing amounts of hPPARδW225A-LBD (0–1.63 μM). These results indicated that the critical amino acid associated with the bi-directional fluorescence properties of **2** is residue 264 located in the omega loop position of hPPARs-LBD. Contrary to our expectation, the change of the side-chain amino acid of hPPARα-LBD 258 residue from leucine to tryptophan did not behave apparently in the same way as wild-type hPPARδ-LBD. The change of the fluorescence intensity of **2** was not significant in the presence of increasing amounts of hPPARαL258W-LBD (0–3.2 μM). Although the exact reason still remain unknown, until now. But FRET is reported to be very sensitive to a distance between the two fluorophore, attenuated depending to the (distance between the two fluorophore).[6] As reported previously, the shapes of the hydrophobic pockets hosting the hydrophobic tail part of the present series of compounds are somewhat different, that is, the hydrophobic pocket of hPPARα-LBD is wider than that of hPPARδ-LBD. Therefore, we speculated that the distance between the two fluorophore is somewhat longer in the case of the binding of **2** complexed with hPPARα-δ L258W-LBD.

3. Conclusion

The fluorescence properties of **2** change in opposite directions upon binding with hPPARδ-LBD and with hPPARα-LBD. The unexpected attenuation in the fluorescence of **2** complexed with hPPARδ-LBD can be attributed to fluorescence energy transfer from the excited-state pyrene to the nearby Trp264 residue of the hPPARδ-LBD. Therefore, it might be possible to create dual-format hPPARδ and hPPARα ligand binding assays simply by utilizing the fluorometric changes elicited by binding of endogenous and/or exogenous ligands. We are now working to construct such a system.

4. Experimental

4.1. Chemistry

4.1.1. Preparation of (*S*)-2-(4-methoxy-3-((pyrene-1-carboxamido)methyl)benzyl) butanoic acid (2)

The preparation of **2** has been reported.[24] The physicochemical properties of **2** used in this study were as follows: ^{1}H NMR (500 MHz, $CDCl_3$) δ 8.46 (d, 1H, J = 9.4 Hz), 8.17 (m, 2H), 7.98 (m, 5H), 7.32 (s, 1H), 7.10 (d, 1H, J = 5.6 Hz), 6.80 (d, 1H, J = 5.6 Hz), 6.63 (m, 1H), 4.70 (m, 2H), 3.82 (s, 3H), 2.87 (m, 1H), 2.74 (m, 1H), 2.56 (m, 1H), 1.50 (m, 2H), 0.94 (t, 3H, J = 7.5 Hz). HRMS; $(M+H)^+$ Calcd for $C_{30}H_{27}NO_4$, 466.2018. Found 466.2029. Anal. Calcd for $C_{30}H_{27}NO_4$: C, 77.40; H, 5.85; N, 3.01. Found: C, 77.24; H, 6.07; N, 3.00. $[\alpha]_D$ 24.6°(c 0.20, MeCN).

4.2. Site-directed mutagenesis

The plasmids encoding wild-type hPPARα and wild-type hPPARδ-LBDs, used as templates for mutagenesis, were the same as those used in the previous crystallographic study.[24] The plasmids pET28a-hPPARαLBD and pET18a-hPPARδ-LBD were generated by cloning DNAs encoding hPPARαLBD (residues 200–468) and hPPARδ-LBD (residues 206–477), respectively, into the pET28a vector (Novagen, Wisconsin, USA). Polymerase chain-reaction (PCR)-mediated mutagenesis was carried out using the QuickChange site-directed mutagenesis kit (Stratagene, California, USA). The forward and reverse primers were complementary and contained the designed nucleotide changes. The primer sequences were as follows (only the forward primers are shown, and the designed changes are indicated by lower-case letters): hPPARαLBD L258W, 5′-TGGTGGCCAAGtgGGTGGCCAATGG-3′; hPPARδLBD-W256A, 5′-GAGACATTGgcGCAGGCAGAGA-3′; hPPARδLBD-W264L, 5′-GGGGCTGGTGctGAAGCAGTTG-3′; hPPARδLBD-W264A, 5′-GGG GCTGGTGgcGAAGCAGTTG-3′. The designed mutations were confirmed by sequencing.

4.3. Purification of wild-type and mutant hPPAR-LBDs

The wild-type and mutant proteins were prepared as described previously.[28] The constructs were expressed as N-terminal His-tagged proteins and purified to homogeneity by means of three steps of column chromatography (HisTrap HP nickel-chelate column (GE Healthcare), HiTrap Q anion-exchange column (GE Healthcare), HiLoad 26/60 Superdex 75 gel-filtration column (GE Healthcare)).The concentrations of the purified wild-type and mutant proteins were as follows: hPPARα-LBD wild, 9.6 mg/mL; hPPARδ-LBD wild, 0.70 mg/mL; hPPARα-LBD L258W, 3.6 mg/mL; hPPARδLBD-W256A, 12 mg/mL; hPPARδLBD-W264L, 0.60 mg/mL; hPPARδLBD-W264A. 0.80 mg/mL.

4.4. Fluorescence measurements

Fluorescence spectra were measured at 25 °C on a Hitachi F2500 spectrofluorophoto-meter with a 1-cm path-length quartz cell. To a 500 nM solution of **2** in binding buffer (Tris–HCl 20 mM, NaCl 150 mM, TCEP (tris[2-carboxyethyl]phosphine hydrochloride)1 mM, pH 7.5) was added 4 μL of each PPAR-LBD solution in a cumulative manner. The system was excited at 345 nM.

Acknowledgment

This work was supported in part by the Targeted Proteins Research Program of the Japan Science and Technology Corporation (JST), the Uehara Memorial Foundation, the Tokyo Biochemical Research Foundation (TBRF) and the Okayama Foundation for Science and Technology (OFST).

References and notes

1. Desvergne, B.; Wahli *Endocrinol. Rev.* **1999**, *20*, 649.
2. Dreyer, C.; Krey, G.; Keller, H.; Givel, F.; Helftenbein, G.; Wahli, W. *Cell* **1992**, *68*, 879.
3. Issemann, I.; Green, S. *Nature* **1990**, *347*, 645.
4. Kota, B. P.; Huang, T. H.; Roufogalis, B. D. *Pharmacol. Res.* **2005**, *51*, 85.
5. Berger, J. P.; Akiyama, T. E.; Meinke, P. T. *Trends Pharmacol. Sci.* **2005**, *26*, 44.
6. Michalik, L.; Auwerx, J.; Berger, J. P.; Chatterjee, V. K.; Glass, C. K.; Gonzalez, F. J.; Grimaldi, P. A.; Kadowaki, T.; Lazar, M. A.; O'Rahilly, S.; Palmer, C. N.; Plutzky, J.; Reddy, J. K.; Spiegelman, B. M.; Staels, B.; Wahli, W. *Pharmacol. Rev.* **2006**, *58*, 726.
7. Banner, C. D.; Göttlicher, M.; Widmark, E.; Sjövall, J.; Rafter, J. J.; Gustafsson, J. A. *J. Lipid Res.* **1993**, *34*, 1583.
8. Nuclear Receptors Nomenclature Committee. *Cell* **1999**, *97*, 1.
9. Wahli, W. *Swiss Med. Wkly.* **2002**, *132*, 83.
10. Mukherjee, R.; Jow, L.; Noonan, D.; McDonnell, D. P. *J. Steroid Biochem Mol. Biol.* **1994**, *51*, 157.
11. Okuno, A.; Tamemoto, H.; Tobe, K.; Ueki, K.; Mori, Y.; Iwamoto, K.; Umesono, K.; Akanuma, Y.; Fujiwara, T.; Horikoshi, H.; Yazaki, Y.; Kadowaki, T. *J. Clin. Invest.* **1998**, *101*, 1354.
12. Braissant, O.; Wahli, W. *Endocrinology* **1998**, *39*, 2748.
13. Lambe, K. G.; Tugwood, J. D. *Eur. J. Biochem.* **1996**, *239*, 1.
14. Vu-Dac, N.; Schoonjans, K.; Laine, B.; Fruchart, J. C.; Auwerx, J.; Staels, B. *J. Biol. Chem.* **1994**, *69*, 31012.
15. Oliver, W. R., Jr.; Shenk, J. L.; Snaith, M. R.; Russell, C. S.; Plunket, K. D.; Bodkin, N. L.; Lewis, M. C.; Winegar, D. A.; Sznaidman, M. L.; Lambert, M. H.; Xu, H. E.; Sternbach, D. D.; Kliewer, S. A.; Hansen, B. C.; Willson, T. M. *Proc. Natl. Acad. Sci. U.S.A.* **2001**, *98*, 5306.
16. Lim, H.; Dey, S. K. *Trends Endocrinol. Metab.* **2000**, *11*, 1372.
17. Peters, J. M.; Lee, S. S.; Li, W.; Ward, J. M.; Gavrilova, O.; Everett, C.; Reitman, M. L.; Hudson, L. D.; Gonzalez, F. J. *Mol. Cell Biol.* **2000**, *20*, 5119.
18. Mano, H.; Kimura, C.; Fujisawa, Y.; Kameda, T.; Watanabe-Mano, M.; Kaneko, H.; Kaneda, T.; Hakeda, Y.; Kumegawa, M. *J. Biol. Chem.* **2000**, *275*, 8126.

19. Ban, S.; Kasuga, J.; Nakagome, I.; Nobusada, H.; Takayama, F.; Hirono, S.; Kawasaki, H.; Hashimoto, Y.; Miyachi, H. *Bioorg. Med. Chem.* **2011**, *19*, 31831.
20. Kasuga, J.; Yamasaki, D.; Araya, Y.; Nakagawa, A.; Makishima, M.; Doi, T.; Hashimoto, Y.; Miyachi, H. *Bioorg. Med. Chem.* **2006**, *14*, 8405.
21. Kasuga, J.; Nakagome, I.; Aoyama, A.; Sako, K.; Ishizawa, M.; Ogura, M.; Makishima, M.; Hirono, S.; Hashimoto, Y.; Miyachi, H. *Bioorg. Med. Chem.* **2007**, *15*, 51770.
22. Kasuga, J.; Yamasaki, D.; Ogura, K.; Shimizu, M.; Sato, M.; Makishima, M.; Doi, T.; Hashimoto, Y.; Miyachi, H. *Bioorg. Med. Chem. Lett.* **2008**, *18*, 1110.
23. Ohashi, M.; Oyama, T.; Nakagome, I.; Sato, M.; Nishio, Y.; Nobusada, H.; Hirono, S.; Morikawa, K.; Hashimoto, Y.; Miyachi, H. *J. Med. Chem.* **2011**, *54*, 331.
24. Araya, Y.; Kasuga, J.; Toyota, K.; Hirakawa, Y.; Oyama, T.; Makishima, M.; Morikawa, K.; Hashimoto, Y.; Miyachi, H. *Chem. Pharm. Bull.* **2008**, *56*, 1357.
25. Oyama, T.; Toyota, K.; Waku, T.; Hirakawa, Y.; Nagasawa, N.; Kasuga, J.; Hashimoto, Y.; Miyachi, H.; Morikawa, K. *Acta Crystallogr., Sect. D Biol. Crystallogr.* **2009**, *65*, 786.
26. Kuwabara, N.; Oyama, T.; Tomioka, D.; Ohashi, M.; Yanagisawa, J.; Shimizu, T.; Miyachi, H. *J. Med. Chem.* **2012**, *55*, 893.
27. Royer, C. A. *Chem Rev.* **2006**, *106*, 1769.
28. Waku, T.; Shiraki, T.; Oyama, T.; Fujimoto, Y.; Maebara, K.; Kamiya, N.; Jingami, H.; Morikawa, K. *J. Mol. Biol.* **2009**, *385*, 188–199.